Low Thermal Conductivity Block from a Hybrid Geopolymer Concrete based on Fly Ash and other Industrial Wastes

Bloque de baja conductividad térmica a partir de un concreto geopolimérico híbrido basado en cenizas volantes y otros residuos industriales

Fabio Martínez-Gutiérrez[1];
William Gustavo Valencia-Saavedra[2];
Ruby Mejía-de-Gutiérrez[3]

[1]Universidad del Valle, Cali – Colombia
fabio.martinez@correounivalle.edu.co
[2]Universidad del Valle, Cali - Colombia
william.gustavo.valencia@correounivalle.edu.co
[3]Universidad del Valle, Cali - Colombia
ruby.mejia@correounivalle.edu.co

How to cite / Cómo citar

Abstract

The use of alternative cementitious materials and the use of industrial waste as supplementary materials or aggregates in the production of concrete and structural elements that guarantee good mechanical performance, reduced dead load, and high thermal comfort are in line with the principles of circular economy in the construction sector. Therefore, the objective of this research was to develop a hybrid cement based on alkaline activation with sodium sulfate (NS) of a mixture of fly ash (CV), silica fume (HS) and ordinary Portland cement (OPC), in proportions (CV+HS)/OPC of 70/30 %. The methodology used consisted of developing the hybrid cementitious material, which was classified as having moderate heat of hydration (MCH type), and subsequently using it, in proportions of 500 and 600 kg/m^3, to produce structural concretes incorporating coarse recycled aggregates (AGR) and fine recycled aggregates (AFR) in the mixture, obtained from construction and demolition waste (CDW). The 600R concrete mixture reached a compressive strength of 18.9 MPa after 28 days of curing and reported a modulus of elasticity of 27 GPa. This concrete was validated in the production of perforated structural blocks, and to improve the thermal comfort of the concrete, 10 % and 20 % of the volume of recycled fine aggregate was replaced with recycled cork. The introduction of cork in the mixture, although it reduces the compressive strength of the block (29 %), allows to reduce the thermal conductivity by 32 %. Based on the results obtained, it is concluded that the use of 10 % of cork volume as a replacement for fine aggregate in the hybrid concrete mix allows the obtaining of a structural block with thermal comfort characteristics. The mixture considered optimal according to the results obtained was composed of 52.5 CV+17.5 HS+30 OPC, 4 % NS, 70 % AGR, 20 % AFR, and 10 % cork.

Keywords

Geopolymer, fly ash, sodium sulfate, structural block, thermal conductivity.

Resumen

La utilización de cementantes alternativos y el aprovechamiento de residuos industriales, como materiales suplementarios o agregados en la producción de concretos y elementos estructurales que garanticen buenas prestaciones mecánicas, disminución de la carga muerta y un elevado confort térmico, están en concordancia con los principios de economía circular en el sector de la construcción. Por ello, el objetivo de esta investigación fue desarrollar un cemento híbrido basado en la activación alcalina con sulfato de sodio (NS) de una mezcla de ceniza volante (CV), humo de sílice (HS) y cemento portland de uso general (OPC, por sus siglas en inglés), en proporciones (CV+HS)/OPC del 70/30 %. La metodología empleada consistió en desarrollar el cementante hibrido, el cual fue clasificado como de moderado calor de hidratación (tipo MCH), y posteriormente utilizarlo, en proporciones de 500 kg/m^3 y 600 kg/m^3 para producir concretos estructurales incorporando en la mezcla agregados reciclados gruesos (AGR) y finos (AFR), obtenidos a partir de residuos de construcción y demolición (RCD). La mezcla 600R a 28 días de curado alcanzó un valor de 18,9 MPa, y reporto un módulo de elasticidad de 27 GPa. Este concreto se validó en la producción de bloques perforados estructurales y, con el fin de mejorar el confort térmico de los concretos, se realizó sustitución del 10 % y 20 % en volumen de agregado fino reciclado por corcho reciclado. La introducción de corcho en la mezcla, aunque redujo la resistencia a compresión del bloque en un 29 %, permitió disminuir la conductividad térmica en un 32 %. Basado en los resultados obtenidos, se concluye que el uso de un 10 % en volumen de corcho como reemplazo del agregado fino en la mezcla de concreto híbrido permite obtener un bloque estructural con características de confort térmico. Las proporciones de la mezcla considerada óptima fueron de 52,5 CV+17,5 HS+30 OPC, 4 % NS, 70 % AGR, 20 % AFR, y 10 % corcho.

Palabras clave

Geopolímero, ceniza volante, sulfato de sodio, bloque estructural, conductividad térmica.

1.   INTRODUCTION

Concrete made from Ordinary Portland Cement (OPC) is one of the most widely used materials in the construction industry. On average, one ton of concrete is produced annually for every person in the world, which underscores the need to consider the environmental impact of its production process, primarily in terms of Greenhouse Gas (GHG) emissions and energy consumption [1]. As a result, recent research has focused on partially or fully replacing cement with alternative binders that contribute to enhanced environmental and energy sustainability. These alternatives include alkali-activated cements and geopolymers, which aim to offer equal or superior performance compared to OPC.

The term *geopolymer,* coined in the 1970s, refers to the chemical reaction product of alkaline silicates and certain aluminosilicate precursors, resulting in the formation of polymeric Si-O-Al bonds [2]. Geopolymers are distinguished for their low permeability, high mechanical strength, and durability (e.g., resistance to elevated temperatures, chemical corrosion, and environmental degradation), among other advantageous properties. Current studies are investigating the mechanisms and reaction kinetics of geopolymer synthesis, as well as the microstructural and mechanical properties of this material. Such studies also explore different types of precursor materials, including fly ash, red mud, biomass ash, metallurgical waste, and recycled glass [3]–[6]. Moreover, over the past 10 years, the study of geopolymer applications has expanded across various fields, including engineering, medicine, mineralogy, geology, colloid science, modern inorganic chemistry, and physical chemistry. Such applications encompass low-cost ceramic materials, sustainable construction solutions, repair materials, protective coatings, thermal insulation, and porous materials [2].

One of the most widely used precursors for geopolymers is Fly Ash (FA), a byproduct of pulverized coal combustion in thermoelectric plants and industrial boilers. This material is considered a hazardous waste, as its release into the environment can result in adverse ecological impacts. Consequently, there is growing interest in developing recycling methods for FA to prevent it from accumulating in landfills or being stored in open environments. One promising application under study is the incorporation of FA into hybrid concretes [7], [8]. For instance, a study was conducted on the production of binders with low heat of hydration [9], utilizing class F (FAF) and class C (FAC) FA to achieve a 70 % OPC replacement by mass. The activating agent used was reagent grade sodium sulfate powder at 3 % or 5 % by mass of the binder, along with a water-to-powder (w/p) ratio of 0.40. The findings indicated that early-age strength was superior for FAC-OPC mixtures compared to FAF-OPC mixtures, with XRD analyses confirming the presence of portlandite and ettringite phases. Other studies have explored solid activator mixtures, such as sodium sulfate with powdered calcium hydroxide, or mixtures of sodium hydroxide and sodium silicate to activate FA in hybrid systems with low OPC content (30–20% by weight). Their results have suggested that the presence of OPC in the mixture favors FA dissolution due to the heat released during the cement hydration, which results in adequate hardening and strength at ambient temperature [10]–[12].

In alignment with circular economy principles, the partial or total replacement of OPC with various supplementary materials—such as FA—not only reduces energy consumption and carbon footprint but also contributes to sustainable fuel, electricity, and natural resource utilization. In addition, the use of Construction and Demolition Waste (CDW) as recycled aggregates, as well as cork waste from the agglomerate industry, is expected to ensure good mechanical performance, reduced dead load, and enhanced thermal comfort in construction applications [6], [13]. Particularly, thermal comfort is influenced by outdoor factors such as climate (humidity, temperature, airflow, solar radiation) and indoor factors like occupants'

physical activity. Therefore, selecting appropriate materials, designing for optimal thermal performance, and constructing an effective building envelope are fundamental considerations.

This applied research project aims to meet the construction industry's current needs while reducing ecological impact, focusing on developing *green* concretes that utilize industrial by-products (non-hazardous industrial waste, NHIW) to minimize the excessive consumption of natural resources. In line with this objective, the project considers the sustainability criteria proposed by the Colombian Council of Sustainable Construction (CCCS), which emphasize efficient material and waste management, as well as maintaining high indoor environmental quality through features such as thermal comfort, the use of alternative raw materials, and the integration of recycled materials to enhance the sustainability of a project [14].

Considering the above, this study set out to develop a hybrid concrete by mixing high percentages of FA with OPC and using a solid activator to produce a hybrid structural geopolymer concrete block that ensures compliance with the property requirements of the NTC 4026 standard [15]. Additionally, this type of concrete was proposed for use in prefabricated materials to ensure thermal comfort in buildings. For this purpose, cork—an industrial by-product with insulating properties—was selected as an additive.

2.   EXPERIMENTAL METHODOLOGY

2.1   Material Selection and Characterization

This study used FA from a local brick plant as a precursor for hybrid alkali-activated systems. The chemical composition of the FA, determined by X-ray fluorescence using a Phillips PANalytical MagiX-Pro PW 2440 spectrometer (4 kW max), is shown in Table 1. The combined content of silicon, aluminum, and iron oxides is approximately 88.98%, which classifies the material as class F FA (minimum 70 %) according to NTC 3493 [16], equivalent to ASTM C618. Table 1 also includes the chemical composition of Silica Fume (SF), used as a replacement for FA, with a high silica content (87.60 %). For the calcium source in producing hybrid systems, general-use OPC was employed, classified as a highly blended cement incorporating limestone.

Table 1. Chemical composition and particle size of FA, OPC, and SF (%). Source: own work.

Component	SiO_2	Al_2O_3	Fe_2O_3	K_2O	CaO	MgO	Na_2O	Others	LOI	Mean particle size (µm)
FA	59.03	23.97	5.98	1.21	0.74	0.31	0.19	2.22	6.35	24.89
OPC	17.99	3.88	4.76	0.32	62.28	1.71	0.23	0.66	8.17	21.65
SF	87.60	0.38	0.66	2.36	0.57	3.67	1.26	0.01	3.49	21.50

The mean particle size D (4.3), determined by laser granulometry using a Mastersizer 2000, was 24.89 µm for FA, 21.50 µm for SF, and 21.65 µm for OPC. Notably, the particle size of SF in this test appears larger than that reported in the product data sheet (0.1 µm), which is due to particle agglomeration during testing. Sodium sulfate (Na_2SO_4) was used as the alkali activator.

Table 2 presents the main characteristics of natural and recycled aggregates obtained from CDW samples. Recycled aggregates exhibited high absorption rates: 8.96 % for recycled fine aggregate (RFA) (NTC 237 [17] equivalent to ASTM C128) and 5.82 % for recycled coarse aggregate (RCA) (NTC 176 [18] equivalent to ASTM C127). RCA had a maximum particle

size of 25.4 mm and the RFA fineness modulus was 3.17 (coarse sand) (NTC 77 [19] equivalent to ASTM C136). RCA had a wear resistance of 28.2 %, which makes it suitable for concrete mixtures (NTC 98 [20] equivalent to ASTM C131). RFA had minimal organic content (organic plate No. 1), favoring its use in mortar and/or concrete mixtures (NTC 127 [21] equivalent to ASTM C40).

Table 2. Physical properties of natural and recycled aggregates. Source: own work.

Physical property	Natural aggregates		Recycled aggregates		Cork
	Fine aggregate NFA	Coarse aggregate NCA	Fine aggregate RFA	Coarse aggregate RCA	
Compact unit mass [kg/m^3]	1643.78	1574.49	1440.37	1520.24	79.89
Voids [%]	33.58	40.88	34.46	34.31	50.56
Loose unit mass [kg/m^3]	1578.55	1443.81	1317.86	1343.94	70.65
Voids [%]	36.21	45.79	40.04	41.93	56.28
Apparent density [g/cm^3]	2.48	2.67	2.20	2.32	0.16
Absorption [%]	3.77	3.25	8.96	5.82	61.87

To produce the reference concrete, based on 100 % OPC, natural aggregates were selected because, unlike recycled aggregates, exhibit low absorption rates (3.8 % for NFA and 3.3 % for NCA), as shown in Table 2. The maximum particle size for NCA was 19 mm, and the fineness modulus for NFA was 2.63. Cork was employed to reduce the thermal conductivity of concrete specimens because it offers a fineness modulus of 3.59 and a notably high absorption rate of 61.87 %.

2.2   Design of Mixtures and Production of Alkali-Activated Materials

Hybrid alkali-activated systems (HAA) were obtained by combining the precursor (FA+SF) and cement (OPC) together with a solution consisting of the alkali activator Na2SO4 (NS) and water. The addition of OPC (30 % by weight) was aimed at avoiding thermal curing in the systems and, as a result, the hybrid systems hardened and developed strengths at ambient temperature.

To evaluate compressive strength at 7 and 28 days of curing, HAA systems were tested by varying NS content within a 2–6 % range and adjusting the SF replacement percentage relative to FA (0–35 % of the total mixture). Strength testing was performed on an INSTRON 3369 universal machine with a capacity of 50 kN and a loading rate of 1 mm/min. Minitab 17 software and a response surface experimental design were employed to determine the optimal proportions of NS and SF within the defined ranges, which resulted in 13 different mixtures, as shown in Table 3. The liquid-to-solid (L/S) ratio for all mixtures was 0.4.

Paste preparation involved a 4-minute mixing cycle in a Hobart mixer, followed by molding into 20 mm cubes. The samples were vibrated for 30 seconds to release air naturally trapped during mixing and molding, then placed in a humid chamber at ambient temperature (25 ± 3°C) for curing. A minimum of three samples per curing age was evaluated for each system.

Table 3. Dosage based on experimental design. Source: own work.

Mixture	Hybrid System			NS activator (% by weight of the activator relative to the total weight of the hybrid system)
	FA (% weight)	SF (% weight)	OPC (% weight)	
1	52.50	17.50	30.00	4.00
2	52.50	17.50	30.00	6.83
3	52.50	17.50	30.00	1.17
4	40.00	30.00	30.00	6.00
5	52.50	17.50	30.00	4.00
6	52.50	17.50	30.00	4.00
7	70.00	0.00	30.00	4.00
8	65.00	5.00	30.00	6.00
9	40.00	30.00	30.00	2.00
10	34.82	35.18	30.00	4.00
11	52.50	17.50	30.00	4.00
12	52.50	17.50	30.00	4.00
13	65.00	5.00	30.00	2.00

Once the optimal proportions for the HAA pastes were determined, the development of compressive strength over a curing period of 1 to 90 days was compared with the results from a paste fully based on general-use OPC.

From the optimal systems, mortars were produced using varying weight ratios of the hybrid system to sand at 1:1, 1:2, and 1:2.75, maintaining a constant liquid-to-solid (L/S) ratio of 0.45 across all systems. These mortars were mixed for 4 minutes using a Hobart mixer, then molded into 50-mm cubes following NTC 112 [22]. Curing took place in a humid chamber at ambient temperature ($25 \pm 3°C$), after which compressive strength was measured at 7 and 28 days using a Controls CT-1500 hydraulic press with a capacity of 1500 kN, in accordance with NTC 220 [23]. Additionally, the setting time was determined following Method B of NTC 118 [24] (equivalent to ASTM C191). Similarly, the heat evolution during alkaline activation and the total heat of reaction over 48 hours were measured using an I-Cal 8000 isothermal calorimeter, in accordance with ASTM C1702.

Following the optimization of HAA, concretes were produced using 100 % recycled aggregates (CHAA-RA) at binder dosages of 500 kg/m³ and 600 kg/m³ (designated as 500R and 600R, respectively). A reference concrete with 600 kg/m³ of HAA and natural aggregates (CHAA-NA, labeled 600N) was also produced. The granulometric combination of fine and coarse aggregates, whether recycled or natural, was maintained at 30 % and 70 %, respectively, by weight. Mixture design was carried out by adapting the *absolute volume method* proposed in ACI 211.1 (see Table 4).

Table 4. Dry mixture design per cubic meter of concrete (1 m³). Source: own work.

Hybrid system	Weight (kg/m³)						
	FA	SF	OPC	NS	Fine aggregate, RFA	Coarse aggregate, RCA	Mixing water
500R	252	84	144	20	383	892	225
600R	302	101	173	24	388	906	270
600N	302	101	173	24	424	990	270

The samples were molded into cylinders of 75 mm diameter and 165 mm height in accordance with NTC 1377 [25]. The specimens were cured in a humidity chamber at room temperature (25 ± 3°C). Once the samples reached curing ages of 7, 28, and 90 days, their compressive strength was evaluated using a Controls CT-1500 hydraulic press with a capacity of 1500 kN, following NTC 673 [26]. The modulus of elasticity was assessed using ultrasonic pulse velocity testing according to ASTM C597 [27], while Indirect Tensile Strength (ITS) was measured at 28 days of curing as per NTC 722 [28]. Moreover, density, absorption, and porosity tests were conducted on the 28-day cured concrete samples following NTC 5653 [29]. Microstructural characterization was performed using Scanning Electron Microscopy (SEM) on a JEOL JSM-6490 LV microscope at an acceleration voltage of 20 kV in low vacuum mode. To this end, samples of 1 cm³ were extracted from the optimal concrete mixture after 28 days of curing, embedded in epoxy resin, and polished on their surfaces.

Finally, using the optimal hybrid concrete mixture with recycled aggregates, perforated blocks were produced using a vibro-compactor. Some blocks incorporated granular cork as a partial replacement (10 % and 20 % by volume) of RFA to improve thermal insulation. These blocks were characterized in accordance with NTC 4024 [30] (equivalent to ASTM C140). The thermal behavior of concrete with and without cork was assessed on samples of 1.5 ± 0.2 mm thickness or height after 28 days of curing, using the Transient Plane Source (TPS) method as per ASTM C518 [31]. This assessment was conducted on a Thermtest Hot Disk TPS 500 S thermal conductivity analyzer which operates in the 0.03 W/mK range to 100 W/mK range. A Kapton 5501 sensor with a radius of 6.403 mm was used with powers of 0.15 W and 0.20 W applied during a measurement time of 40 seconds at a working temperature of 25 ± 0.5°C. This process aimed to determine whether the incorporation of cork enhances the thermal insulation properties of concrete.

3.   RESULTS AND ANALYSIS

3.1   Characterization of Hybrid Cement Based on FA-SF

Figure 1 presents contour plots derived from the strength results of the mixtures listed in Table 3. This figure illustrates the effect of NS weight percentage on compressive strength in relation to the incorporation of SF. At 7 days of curing (Figure 1a), the highest strengths are achieved with NS percentages between 2.5 % and 4.2 % and SF content between 15 % and 20 %, reaching compressive strength values of 15 MPa. After 28 days, (Figure 1b), the maximum strengths (19 MPa) occur with NS percentages between 0 % and 2 % and SF content between 25 % and 35 % by weight as a replacement for FA. The results suggest that the presence of SF promotes increased compressive strength, which may be due to its contribution of amorphous silica. This silica reacts with the calcium hydroxide formed during cement hydration, producing Calcium Silicate Hydrate (CSH) [32]–[34]. Additionally, the particle size of SF enhances paste densification [35], [36].
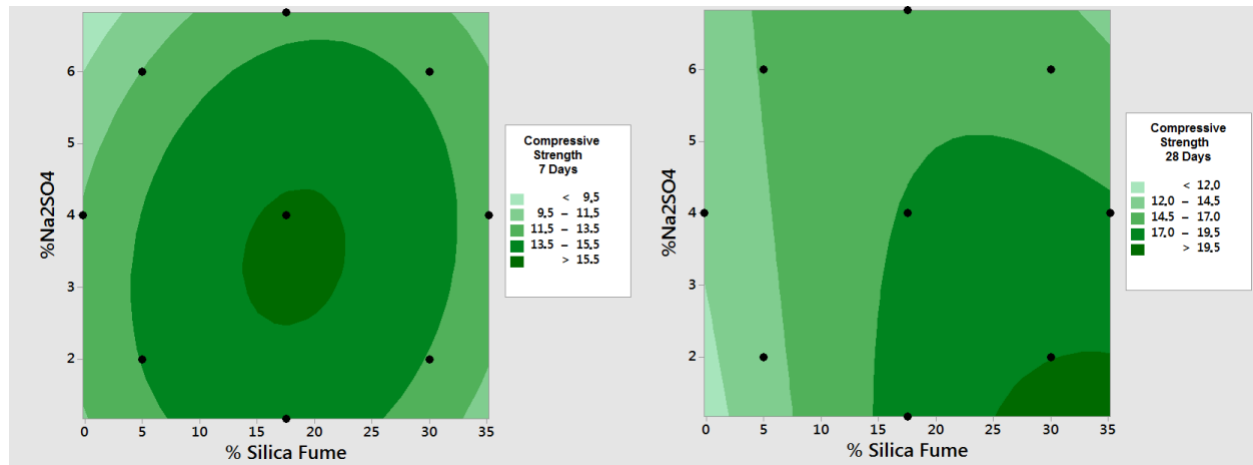
Figure 1. Contour plots for weight percentage of NS and SF: (a) 7 days of curing; (b) 28 days of curing.
Source: own work.

Based on the reported results, two HAA systems were selected as optimal. For the 7-day compressive strength results, the selected mixture consisted of 52.50 % FA, 17.50 % SF, 30 % OPC, and 4 % NS (HAA-1). For the 28-day results, the optimal mixture included 40 % FA, 30 % SF, 30 % OPC, and 2 % NS (HAA-2) (Figure 1). The NS dosages in these mixtures are consistent with previous studies that recommend NS values between 1 % and 5 % by weight [8], [37]–[39].

Figure 2 illustrates the compressive strength development of the optimal systems (HAA-1 and HAA-2) compared to the 100 % OPC reference mixture. An increase in compressive strength is observed across all samples as the curing time progresses. While HAA-1 exhibits the highest compressive strength at 7 days, followed by HAA-2, the reference sample surpasses them in strength at later ages. In general, the compressive strength values for HAA-1 and HAA-2 remain similar across the different curing ages evaluated.

For its part, Figure 3 shows the compressive strength of mortars produced from HAA-1 and HAA-2 with a water-to-solid (W/S) ratio of 0.45 and various hybrid cement system-to-sand ratios at 7 and 28 days of curing, with the dosages specified in Table 5.

Across all systems, compressive strength decreases as the cement-to-sand ratio increases. However, it consistently increases from 7 to 28 days of curing. Specifically, for HAA-1, compressive strength increases by 12 %, 27 %, and 24 % at cement-to-sand ratios of 1:1, 1:2, and 1:2.75, respectively. For HAA-2, these increases are 34 %, 29 %, and 5 % at the same ratios. Considering these results, HAA-1 was selected for producing the concrete mixtures, as it exhibited higher compressive strengths at most cement-to-sand ratios and curing ages. In addition, the proportion of SF is lower [35], [40]–[42].

Table 5. Dosages of mortar mixtures for optimal systems incorporating SF and varying hybrid cement system-to-sand ratios. Source: own work.

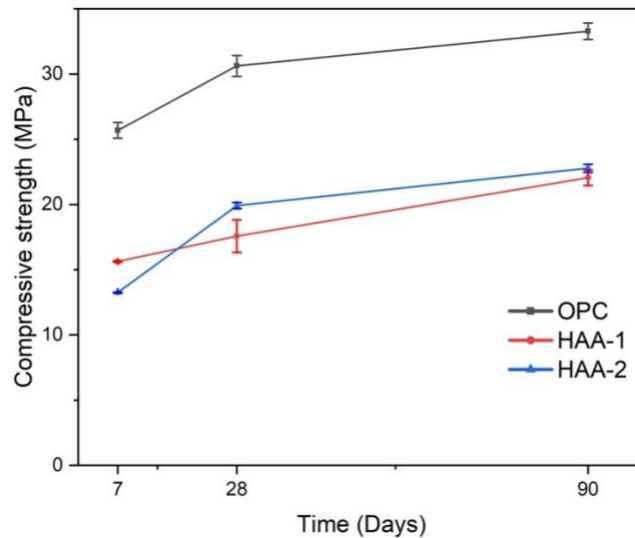| Cement-to-sand ratio	HAA-1		HAA-2	
	SF (% weight)	NS (% weight)	SF (% weight)	NS (% weight)
1:1	17.50	4.00	30.00	2.00
1:2	17.50	4.00	30.00	2.00
1:2.75	17.50	4.00	30.00	2.00

Figure 2. Evolution of the average compressive strength in optimal hybrid systems incorporating SF, compared to the 100 % OPC sample. Source: own work.

The initial and final setting times for the HAA-1 paste were 108 and 360 minutes, respectively. This paste consisted of 52.5 % FA, 17.5 % SF, and 30 % OPC, activated with 4 % NS and a W/S ratio of 0.45. Figure 4 illustrates the heat flow of HAA-1. By determining the area under the curve, a total accumulated heat of 106 kJ/kg was obtained, which is lower than that reported for 100 % OPC systems, where values often exceed 200 kJ/kg [6], [8]. According to these results, the hybrid activated cement HAA-1 can be classified as a moderate heat of hydration cement (type MHC) according to NTC 121 [43]. This classification considers the initial setting time of 108 minutes and the 7-day compressive strength of 12.2 MPa in mortars with a cement-to-sand ratio of 1:2.75.
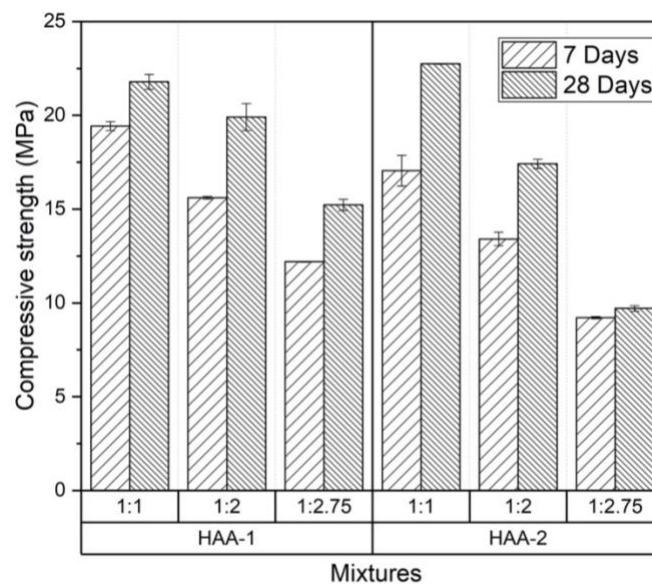

Figure 3. Average compressive strength at 7 and 28 days of curing for the optimal systems HAA-1 and HAA-2 with different cement-to-sand ratios. Source: own work.
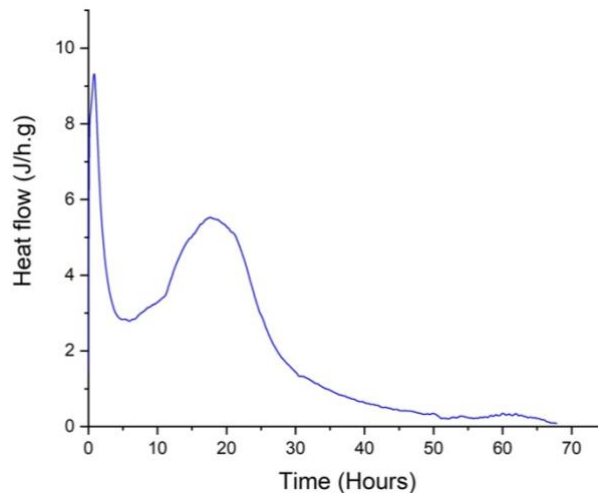
Figure 4. Heat evolution curve for HAA-1. Source: own work.

3.2 Characterization of Hybrid Concrete (CHAA) Based on FA and SF Using Recycled Aggregates

Figure 5 presents the compressive strengths of the hybrid concretes made with two HAA-1 cementitious agent proportions (500R and 600R) using 100 % recycled aggregates, along with the reference hybrid concrete containing natural aggregates (600N). In all evaluated concretes, compressive strength increased with curing time, a characteristic typical of Portland cement-based concretes. Notably, there is a significant difference in compressive strength between concretes with 600 kg/m³ of HAA-1 and those with 500 kg/m³. This increase in the 600R concrete's strength is attributed to its higher cementitious content, leading to the formation of a greater volume of C-S-H, C-A-S-H, and (N,C)-A-S-H gels. At 28 days of curing, the 600R mix achieved a compressive strength of 18.9 MPa, surpassing by 11 % the minimum requirement of 17 MPa for structural concrete, as specified in Title C of Colombia's Seismic Resistant Construction Regulation NSR-10 [44], based on the Regulation Requirements for Structural Concrete, ACI 318S-19 [45]. In contrast, the 500R mix reached a compressive strength of 15.6 MPa at 28 days, which is 8 % lower than the NSR-10 standard's minimum requirement.

It is also notable that the HAA-1 600R mix reported superior compressive strength compared to the hybrid mixture with natural aggregates (600N), which achieved a compressive strength of only 16.3 MPa at 28 days. This enhanced performance could be due to the reactive potential of certain recycled aggregate components (CDW), particularly the finer fractions. These components may react with the activator and partially contribute as binders in the geopolymerization process, thereby densifying the mixture and improving its mechanical strength [6], [46]–[48].

The results from the ITS tests of the concrete mixtures at 28 days of curing are presented in Table 6. The 600R mixture demonstrates a higher ITS, with an average value of 1.5 MPa, compared to the 500R and 600N mixtures. This increase in ITS for 600R may be due to enhanced adhesion between the recycled aggregates and the cement matrix. These ITS results align with the trends observed in compressive strength, showing consistent behavior across these tests.

Table 8 presents the results of physical property evaluations, including bulk density, absorption percentage, and porosity, for concrete mixtures at 28 days of curing, in accordance with NTC 5653 [29]. The bulk density values align with those typically reported for conventional OPC concretes. 600N exhibits the highest density among the three mixtures (2680 kg/m³), attributed to the higher density of natural aggregates versus recycled aggregates.
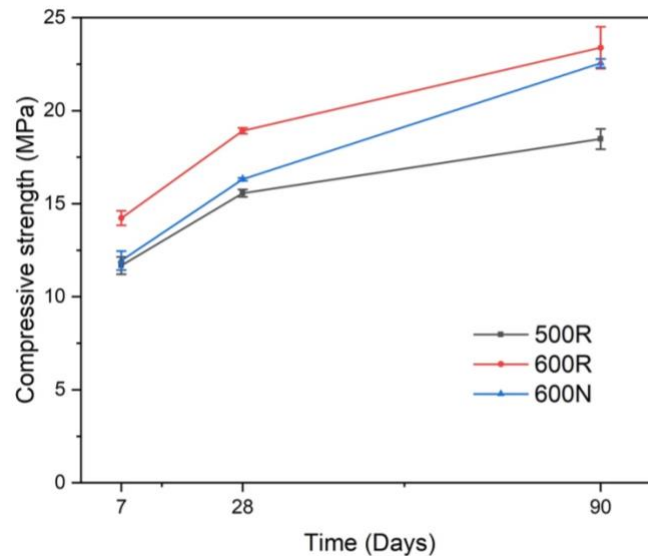
Figure 5. Compressive strength of hybrid concrete mixtures incorporating recycled aggregates at 7, 28, and 90 days of curing, with varying amounts of cementitious agent. Source: own work.

Table 7 displays the results of the modulus of elasticity test for the concrete mixtures at 28 days of curing. To calculate the modulus of elasticity by the ultrasonic pulse method, ASTM C597 requires a Poisson's ratio. Based on NSR-10 recommendations and literature values for geopolymer concretes derived from FA (ranging between 0.192 and 0.203), a value of 0.2 was selected as appropriate. Increasing the hybrid cementitious agent proportion raised the modulus of elasticity from 25.1 GPa for 500R to 27.0 GPa for 600R. However, the 600N mixture shows an even higher modulus (27.6 GPa), likely attributable to the distinct characteristics of natural aggregates.

Table 1. Average <u>indirect tensile strength of concrete mixtures at 28 days of curing</u>. Source: own work.

Amounts (kg/m^3)	Average indirect tensile strength (MPa)
	28 days
500R	1.0 ± 0.1
600R	1.5 ± 0.1
600N	1.3 ± 0.3

Table 2. Results of the modulus of elasticity test on concrete mixtures. Source: own work.

Modulus of elasticity	Average V (m/s)	Average t (s)	Average E (GPa)
Sample			
500R	3270.89	46.55	25.1
600R	3414.00	44.53	27.0
600N	3383.78	45.02	27.6

For the recycled aggregate mixtures, 600R has a higher density (2610 kg/m^3) than 500R (2570 kg/m^3). Concretes made with recycled aggregates display increased absorption, which is consistent with prior aggregate absorption results and corroborates findings from other studies [53]–[57]. A similar behavior is observed in the void volume percentage in the 500R and 600R mixtures. Overall, the concretes with natural aggregates demonstrate superior performance, with lower absorption and void volumes.

Table 8. Results of density, absorption, and porosity tests on concrete mixtures at 28 days of curing. Source: own work.

Mixture	Absorption (%)	Bulk density (kg/m^3)	Void volume (%)
500R	20.79	2570	35.11
600R	18.79	2610	32.59
600N	12.99	2680	25.80

The microstructural analysis of the 600R concrete was conducted using SEM. As shown in Figure 6a, the surface is dense and homogeneous with low porosity. In the aggregate-matrix interface zone, the matrix demonstrates good densification, with strong adhesion visible between the concrete phases (Figure 6b), corroborating the favorable mechanical behavior observed previously.
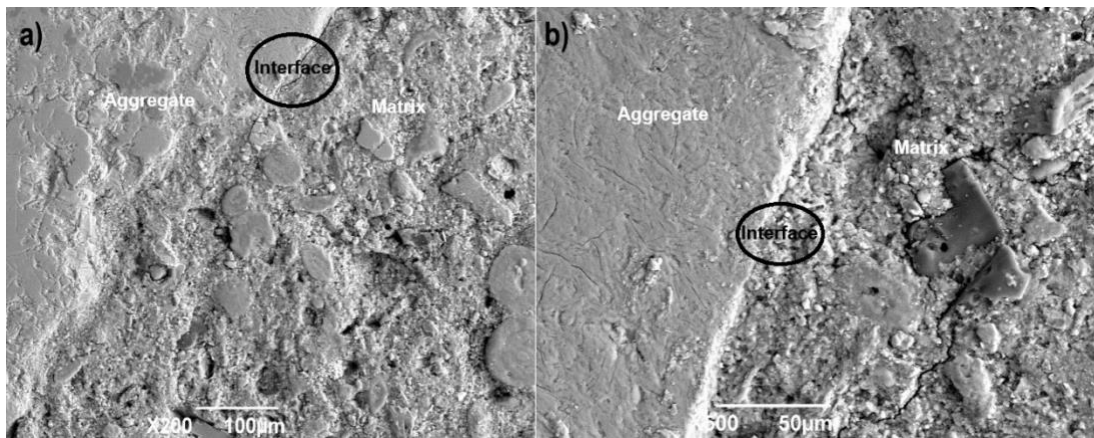
Figure 6. Microstructure of 600R concrete: (a) 100 µm and (b) 50 µm. Source: own work.

3.3 Production and Characterization of a Perforated Block from CHAA with Cork Replacement

Perforated blocks were manufactured from CHAA-600R concrete (Figure 7), replacing RFA with cork at 10 % and 20 % by volume for CHAA-F1 and CHAA-F2, respectively. The results of their characterization were compared with those of the reference block without cork (CHAA-F0), which contained 100 % RFA. Physical and mechanical test followed NTC 4024, NTC 4026, and NTC 4076 standards [30], [15], [58]. Table 9 lists the requirements for structural and non-structural block classification.

Figure 7. Blocks released from the vibro-compactor. Source: own work.

Table 9. Requirements for compressive strength, water absorption, and weight classification of concrete units for structural and non-structural masonry (N-S) according to NTC 4026 [15] and NTC 4076 [58]. Source: own work.

Compressive strength at 28 days, evaluated on average net area		Water absorption % by weight (density) of kiln-dried concrete, kg/m³		
Minimum, MPa		Average of 3 units, maximum, %		
Class	Average of 3 units	Light weight, < 1680 kg/m³	Medium weight, 1680–2000 kg/m³	Normal weight, ≥ 2000 kg/m³
High	13	15	12	9
Low	8	18	15	12
NS	6	18	15	12

Table 10 presents the properties and characteristics of the perforated blocks. Notably, the 28-day compressive strength of CHAA-F0 reached 10.2 MPa, exceeding the NTC 4026 threshold of 8 MPa for *Low-Class Structural Block* classification by 27 %. For CHAA-F1 and CHAA-F2, the compressive strengths were 7.2 MPa and 6.2 MPa, respectively, classifying them as non-structural elements [58]. The observed decrease in compressive strength with increased cork volume aligns with prior findings, where cork addition leads to diminished mechanical properties [13], [59].

As shown in prior results, concretes produced with the alkali-activated system continue to significantly increase their compressive strength at prolonged curing ages. Accordingly, block performance was re-evaluated at 90 days. For the CHAA-F0 block, the 90-day compressive strength qualifies it as a *High-Class Structural Block* per NTC 4026 requirements. Meanwhile, CHAA-F1 and CHAA-F2 met *Low-Class Structural Block* criteria, with compressive strengths of 11.6 MPa and 9.6 MPa, respectively, surpassing the minimum requirement by up to 45 %.

According to NTC 4026, the allowable maximum water absorption for medium-weight blocks (1680–2000 kg/m³) is 15 %. However, all three block types demonstrated absorption rates of approximately 17 %, likely due to the use of recycled aggregates (CDW). It should be noted that NTC 4024 establishes that these water absorption and compressive strength limits must be achieved within 12 months after production, a feasible target given the ongoing improvement in mechanical properties and material densification. The results at both 28 and 90 days affirm the suitability of CHAA for prefabricated construction applications.

Table 3. Block properties obtained at 28 days of curing, following the standards NTC 4026 [15] and NTC 4076 [58]. Source: own work.

Block	% cork by volume, (Replacement of fine aggregate)	Compressive strength (MPa)		Dry density (kg/m³)	Absorption (%)	Humidity (%)
		28 days	90 days			
F0	0	10.2 ± 1.7	13.0	1785.51	17.16	6.67
F1	10	7.2 ± 0.9	11.6	1759.86	17.58	6.99
F2	20	6.2 ± 1.2	9.6	1759.22	17.04	7.19

3.4   Evaluation of the Effect of Cork Incorporation on Thermal Behavior of Concrete

Table 11 presents the thermal properties of concrete containing 600 kg/m^3 of HAA-1 cementitious agent, specifically for mixtures with natural aggregates (CHAA-F0N), recycled aggregates (CHAA-F0R), and recycled aggregates partially replaced by cork at 10 % and 20 % (CHAA-F1 and CHAA-F2, respectively). Moreover, the volumetric heat capacity was calculated by multiplying each sample's density by its specific heat.

Table 4. Thermal properties of the samples at 28 days of curing. Source: own work.

Sample	Cork (%)	Thermal conductivity (W/mK)	Thermal diffusivity (mm^2/s)	Volumetric heat capacity (MJ/m^{3}K)
F0N	0	1.0888	0.8238	1.3337
F0R	0	1.0267	0.8035	1.3050
F1	10	0.6934	0.6290	1.1044
F2	20	0.7239	0.5829	1.2420

The F0N concrete sample, containing natural aggregates, exhibited the highest thermal conductivity and diffusivity. This may be due to the lower porosity of natural aggregates, which allows for more efficient heat transmission. In comparison, samples with recycled aggregates and cork replacements showed reductions in thermal conductivity of 5 %, 36 %, and 33 % for F0R, F1, and F2 concretes, respectively. The thermal diffusivity results follow a similar trend, with F1 and F2 concretes displaying the lowest values. Specifically, comparing F0R with F1 and F2 shows a reduction in thermal conductivity of 32 % and 29 %, respectively. These results confirm that adding cork reduces thermal conductivity, which aligns with a corresponding reduction in mechanical strength, consistent with findings in previous studies [13], [59].

4.   CONCLUSIONS

The results of this study demonstrate that it is feasible to produce a structural-grade block from a hybrid geopolymer concrete activated with 4 % NS and based on FA by combining 52.5 FA+17.5 SF+30 OPC and using recycled aggregates derived from CDW.

The early-age compressive strengths (7 days) of the hybrid concretes ranged from 12 MPa to 15 MPa—satisfactory for a geopolymeric material based on FA, containing minimal OPC, activated by NS, and incorporating recycled aggregates.

This eco-product, with its use of industrial by-products, alternative solid activator, minimal OPC content, and room-temperature curing, suggests a lower carbon footprint compared to traditional structural blocks made from 100 % OPC with natural aggregates or baked clay.

The addition of cork to the sample, while reducing compressive strength, enhances thermal properties. Importantly, the strength of these alkali-activated materials continues to increase over time. Thus, after 90 days, blocks with cork additions progressed from a non-structural to a structural classification, meeting the required standards for structural blocks.

Therefore, incorporating 10 % cork by volume as a fine aggregate replacement is recommended to achieve a structural block with improved thermal comfort.

5.   ACKNOWLEDGMENTS AND FUNDING

CONFLICTS OF INTEREST

The authors declare no economic, professional, or personal conflicts of interest that could unduly influence the results presented in this article.

AUTHOR CONTRIBUTIONS

Fabio Martínez-Gutiérrez: Research design and execution, manuscript drafting, and final review.
William Gustavo Valencia-Saavedra: Conceptualization, supervision, research design, manuscript drafting, and final review.
Ruby Mejía de Gutiérrez: Conceptualization, research design, supervision, manuscript drafting, and final review.

6.   REFERENCES

[1]   P. V. Den Heede, and N. De Belie, "Environmental impact and life cycle assessment (LCA) of traditional and 'green' concretes: Literature review and theoretical calculations," *Cem. Concr. Compos.*, vol. 34, no. 4, pp. 431–442, Apr. 2012. https://doi.org/10.1016/j.cemconcomp.2012.01.004

[2]   Y. Wu *et al.*, "Geopolymer, green alkali activated cementitious material: Synthesis, applications and challenges," *Construction and Building Materials,* vol. 224, pp. 930–949, Nov. 2019. https://doi.org/10.1016/j.conbuildmat.2019.07.112

[3]   J. L. Provis, A. Palomo, and C. Shi, "Advances in understanding alkali-activated materials," *Cement and Concrete Research*, vol. 78, pp. 110–125, Dec. 2015. https://doi.org/10.1016/j.cemconres.2015.04.013

[4]   O. Rojas-Duque, L. M. Espinosa, R. A. Robayo-Salazar, and R. Mejía de Gutiérrez, "Alkali-activated hybrid concrete based on fly ash and its application in the production of high-class structural blocks," *Crystals (Basel)*, vol. 10, no. 10, p. 946, Oct. 2020. https://doi.org/10.3390/cryst10100946

[5]   M. A. Villaquirán-Caicedo, "Studying different silica sources for preparation of alternative waterglass used in preparation of binary geopolymer binders from metakaolin/boiler slag," *Construction and Building Materials,* vol. 227, p. 116621, Dec. 2019. https://doi.org/10.1016/j.conbuildmat.2019.08.002

[6]   R. A. Robayo-Salazar, W. Valencia-Saavedra, and R. M. de Gutiérrez, "Construction and demolition waste (Cdw) recycling—as both binder and aggregates—in alkali-activated materials: A novel re-use concept," *Sustainability,* vol. 12, no. 14, p. 5775, Jul. 2020. https://doi.org/10.3390/su12145775

[7]   Z. T. Yao *et al.*, "A comprehensive review on the applications of coal fly ash," *Earth-Science Reviews*, vol. 141, pp. 105–121, Feb. 2015. https://doi.org/10.1016/j.earscirev.2014.11.016

[8]   W. Valencia-Saavedra, R. Robayo-Salazar, and R. M. de Gutiérrez, "Alkali-activated hybrid cements based on fly ash and construction and demolition wastes using sodium sulfate and sodium carbonate," *Molecules*, vol. 26, no. 24, Dec. 2021. https://doi.org/10.3390/molecules26247572

[9]   A. Dakhane, S. Tweedley, S. Kailas, R. Marzke, and N. Neithalath, "Mechanical and microstructural characterization of alkali sulfate activated high volume fly ash binders," *Materials & Design,* vol. 122, pp. 236–246, May. 2017. https://doi.org/10.1016/j.matdes.2017.03.021

[10]   A. Fernández-Jiménez, I. García-Lodeiro, S. Donatello, O. Maltseva, and Á. Palomo, "Specific examples of hybrid alkaline cement," *MATEC Web of Conferences*, vol. 11, p. 01001, Apr. 2014. https://doi.org/10.1051/matecconf/20141101001

[11]   I. García-Lodeiro, A. Fernández-Jiménez, and A. Palomo, "Variation in hybrid cements over time. Alkaline activation of fly ash-portland cement blends," *Cement and Concrete Research,* vol. 52, pp. 112–122, Oct. 2013. https://doi.org/10.1016/j.cemconres.2013.03.022

[12]   I. Wilińska, B. Pacewska, and A. Ostrowski, "Investigation of different ways of activation of fly ash–cement mixtures: Part 1. Chemical activation by Na2SO4 and Ca (OH)$_2$," *Journal of Thermal Analysis and Calorimetry,* vol. 138, no. 6, pp. 4203–4213, Dec. 2019. https://doi.org/10.1007/s10973-019-08485-1

[13]   R. M. Novais, L. Senff, J. Carvalheiras, M. P. Seabra, R. C. Pullar, and J. A. Labrincha, "Sustainable and efficient cork - inorganic polymer composites: An innovative and eco-friendly approach to produce ultra-lightweight and low thermal conductivity materials," *Cement and Concrete Composites,* vol. 97, pp. 107–117, Mar. 2019. https://doi.org/10.1016/j.cemconcomp.2018.12.024

[14]   Ministerio de Ambiente y Desarrollo Sostenible, "Construcción sostenible," minambiente.gov.co, Accessed: Feb. 20, 2024. [Online.] Available: https://www.minambiente.gov.co/asuntos-ambientales-sectorial-y-urbana/construccion-sostenible/

[15]   NTC 4026, Ingeniería civil y arquitectura. Unidades (bloques y ladrillos) de concreto, para mampostería estructural, ICONTEC - Instituto Colombiano de Normas Técnicas, Bogotá, Colombia, 1997. [Online]. Available: https://tienda.icontec.org/gp-ingenieria-civil-y-arquitectura-unidades-bloques-y-ladrillos-de-concreto-para-mamposteria-estructural-ntc4026-1997.html

[16]   NTC 3493, Cenizas volantes y puzolanas naturales, calcinadas o crudas, para uso en el concreto, ICONTEC - Instituto Colombiano de Normas Técnicas, Bogotá, Colombia, 2019. [Online]. Available: https://tienda.icontec.org/gp-ntc-cenizas-de-carbon-y-puzolanas-naturales-calcinadas-o-crudas-para-uso-en-el-concreto-ntc3493-2023.html

[17]   NTC 237, Método de ensayo para determinar la densidad relativa (gravedad específica) y la absorción del agregado fino, ICONTEC - Instituto Colombiano de Normas Técnicas, Bogotá, Colombia, 2020. [Online]. Available: https://tienda.icontec.org/gp-metodo-de-ensayo-para-determinar-la-densidad-relativa-gravedad-especifica-y-la-absorcion-del-agregado-fino-ntc237-2020.html

[18]   NTC 176, Método de ensayo para determinar la densidad relativa (gravedad específica) y la absorción del agregado grueso, ICONTEC - Instituto Colombiano de Normas Técnicas, Bogotá, Colombia, 2019. [Online]. Available: https://tienda.icontec.org/gp-metodo-de-ensayo-para-determinar-la-densidad-relativa-gravedad-especifica-y-la-absorcion-del-agregado-grueso-ntc176-2019.html

[19]   NTC 77, Concretos. Método de ensayo para el análisis por tamizado de los agregados finos y gruesos, ICONTEC - Instituto Colombiano de Normas Técnicas, Bogotá, Colombia, 2018. [Online]. Available: https://tienda.icontec.org/gp-concretos-metodo-de-ensayo-para-el-analisis-por-tamizado-de-los-agregados-finos-y-gruesos-ntc77-2018.html

[20]   NTC 98, Método de ensayo para determinar la resistencia al desgaste por abrasión e impacto de agregados gruesos menor de 37,5 mm, utilizando la máquina de los ángeles, ICONTEC - Instituto Colombiano de Normas Técnicas, Bogotá, Colombia, 2019. https://tienda.icontec.org/gp-metodo-de-ensayo-para-determinar-la-resistencia-al-desgaste-por-abrasion-e-impacto-de-agregados-gruesos-menor-de-375-mm-utilizando-la-maquina-de-los-angeles-ntc98-2019.html

[21]   NTC 127, Concretos. Método de ensayo para determinar las impurezas orgánicas en agregado fino para concreto, ICONTEC - Instituto Colombiano de Normas Técnicas, Bogotá, Colombia, 2000. [Online]. Available: https://tienda.icontec.org/gp-concretos-metodo-de-ensayo-para-determinar-las-impurezas-organicas-en-agregado-fino-para-concreto-ntc127-2000.html

[22]   NTC 112, Cementos. Mezcla mecánica de pastas y morteros de cemento hidráulico de consistencia plástica, ICONTEC - Instituto Colombiano de Normas Técnicas, Bogotá, Colombia, 2021. [Online]. Available: https://tienda.icontec.org/gp-cementos-mezcla-mecanica-de-pastas-y-morteros-de-cemento-hidraulico-de-consistencia-plastica-ntc112-2021.html

[23]   NTC 220, Cementos. Determinación de la resistencia de morteros de cemento hidráulico a la compresión, usando cubos de 50 mm o 2 pulgadas de lado, ICONTEC - Instituto Colombiano de Normas Técnicas, Bogotá, Colombia, 2021. https://tienda.icontec.org/gp-ntc-cementos-determinacion-de-la-resistencia-de-morteros-de-cemento-hidraulico-a-la-compresion-usando-cubos-de-50-mm-o-2-pulgadas-de-lado-ntc220-2022.html

[24]   NTC 118, Cementos. Método de ensayo para determinar el tiempo de fraguado del cemento hidráulico mediante aguja de Vicat, ICONTEC - Instituto Colombiano de Normas Técnicas, Bogotá, Colombia, 2000. [Online]. Available:

https://tienda.icontec.org/gp-ntc-cementos-metodo-de-ensayo-para-determinar-el-tiempo-de-fraguado-del-cemento-hidraulico-mediante-aguja-de-vicat-ntc118-2022.html

[25]   NTC 1377, Ingeniería civil y arquitectura. Elaboración y curado de especímenes de concreto para ensayos en el laboratorio, ICONTEC - Instituto Colombiano de Normas Técnicas, Bogotá, Colombia, 2010. [Online]. Available: https://tienda.icontec.org/gp-ntc-concretos-elaboracion-y-curado-de-especimenes-de-concreto-para-ensayos-en-el-laboratorio-ntc1377-2021.html

[26]   NTC 673, Concretos. Ensayo de resistencia a la compresión de especímenes cilíndricos de concreto, ICONTEC - Instituto Colombiano de Normas Técnicas, Bogotá, Colombia, 2010. [Online]. Available: https://tienda.icontec.org/gp-concretos-metodo-de-ensayo-de-resistencia-a-la-compresion-de-especimenes-cilindricos-de-concreto-ntc673-2021.html

[27]   C09 Committee, Test method for pulse velocity through concrete, ASTM International, West Conshohocken, PA, 2023. [Online]. Available: https://doi.org/10.1520/C0597-22

[28]   NTC 722, Concreto. Método de ensayo para determinar la resistencia a la tensión indirecta de especímenes cilíndricos de concreto, ICONTEC - Instituto Colombiano de Normas Técnicas, Bogotá, Colombia, 2000. [Online]. Available: https://tienda.icontec.org/gp-ntc-concretos-metodo-de-ensayo-para-determinar-la-resistencia-a-la-tension-indirecta-de-especimenes-cilindricos-de-concreto-ntc722-2021.html

[29]   NTC 5653, Determinación de la gravedad especifica, absorción y vacíos en el concreto endurecido, ICONTEC - Instituto Colombiano de Normas Técnicas, Bogotá, Colombia, 2008. [Online]. Available: https://tienda.icontec.org/gp-determinacion-dela-gravedad-especifica-absorcion-y-vacios-en-el-concreto-endurecido-ntc5653-2008.html

[30]   NTC 4024, Prefabricados de concreto. Muestreo y ensayo de prefabricados de concreto no reforzados, vibrocompactados, ICONTEC - Instituto Colombiano de Normas Técnicas, Bogotá, Colombia, 2001. [Online]. Available: https://tienda.icontec.org/gp-ntc-prefabricados-de-concreto-muestreo-y-ensayo-de-prefabricados-de-concreto-no-reforzados-vibrocompactados-ntc4024-2001.html

[31]   ASTM C518-21: Standard Test Method for Steady-State Thermal Transmission Properties by Means of the Heat Flow Meter Apparatus, ASTM-American Society for Testing and Materials, Pensilvania, Estados Unidos, 2021. https://standards.iteh.ai/catalog/standards/astm/fcd5f52a-9dd7-431d-a171-1e83f99aa51f/astm-c518-21?srsltid=AfmBOop_M1xwYqveTaVkRl9KGNyGmC2ScIGY9pO2Pzjz1q8tnQtHWiQZ

[32]   R. Siddique, "Utilization of silica fume in concrete: Review of hardened properties," Re*sources, Conservation and Recycling* vol. 55, no. 11. pp. 923–932, Sep. 2011. https://doi.org/10.1016/j.resconrec.2011.06.012

[33]   M. Nili, and A. Ehsani, "Investigating the effect of the cement paste and transition zone on strength development of concrete containing nanosilica and silica fume," *Materials & Design,* vol. 75, pp. 174–183, Jun. 2015. https://doi.org/10.1016/j.matdes.2015.03.024

[34]   D. Siang Ng *et al.*, "Influence of SiO_2, TiO_2 and Fe_2O_3 nanoparticles on the properties of fly ash blended cement mortars," *Construction and Building Materials,* vol. 258, p. 119627, Oct. 2020. https://doi.org/10.1016/j.conbuildmat.2020.119627

[35]   A. Mehta, and D. K. Ashish, "Silica fume and waste glass in cement concrete production: A review," *Journal of Building Engineering*, vol. 29, p.100888, May. 2020. https://doi.org/10.1016/j.jobe.2019.100888

[36]   Y. Yue, J. J. Wang, and Y. Bai, "Tracing the status of silica fume in cementitious materials with Raman microscope," *Construction and Building Materials,* vol. 159, pp. 610–616, Jan. 2018. https://doi.org/10.1016/j.conbuildmat.2017.11.015

[37]   G. Yang, T. Wu, C. Fu, and H. Ye, "Effects of activator dosage and silica fume on the properties of Na2SO4-activated high-volume fly ash," *Construction and Building Materials,* vol. 278, p. 122346, Apr. 2021. https://doi.org/10.1016/j.conbuildmat.2021.122346

[38]   J. Mei *et al.*, "Effect of sodium sulfate and nano-SiO2 on hydration and microstructure of cementitious materials containing high volume fly ash under steam curing," *Construction and Building Materials,* vol. 163, pp. 812–825, Feb. 2018. https://doi.org/10.1016/j.conbuildmat.2017.12.159

[39]   D. F. Velandia, C. J. Lynsdale, J. L. Provis, F. Ramirez, and A. C. Gomez, "Evaluation of activated high volume fly ash systems using Na2SO4, lime and quicklime in mortars with high loss on ignition fly ashes," *Construction and Building Materials,* vol. 128, pp. 248–255, Dec. 2016. https://doi.org/10.1016/j.conbuildmat.2016.10.076

[40]   M. Saridemir, "Effect of silica fume and ground pumice on compressive strength and modulus of elasticity of high strength concrete," *Construction and Building Materials,* vol. 49, pp. 484–489, Dec. 2013. https://doi.org/10.1016/j.conbuildmat.2013.08.091

[41]   M. Mazloom, A. A. Ramezanianpour, and J. J. Brooks, "Effect of silica fume on mechanical properties of high-strength concrete," *Cement and Concrete Composites,* vol. 26, no. 4, pp. 347–357, May. 2004.

https://doi.org/10.1016/S0958-9465(03)00017-9

[42]   S. M. Motahari Karein, A. A. Ramezanianpour, T. Ebadi, S. Isapour, and M. Karakouzian, "A new approach for application of silica fume in concrete: Wet granulation," *Construction and Building Materials,* vol. 157, pp. 573–581, Dec. 2017. https://doi.org/10.1016/j.conbuildmat.2017.09.132

[43]   NTC 121, Especificación de desempeño para cemento hidráulico, ICONTEC - Instituto Colombiano de Normas Técnicas, Bogotá, Colombia, 2021. [Online]. Available: https://tienda.icontec.org/gp-especificacion-de-desempeno-para-cemento-hidraulico-ntc121-2021.html

[44]   NSR-10, Reglamento Colombiano de construcción sismo resistente, Ministerio de Ambiente, Vivienda y Desarrollo Territorial-Asociación Colombiana de ingeniería sísmica, Bogotá, Colombia, 2010. [Online]. Available: https://www.unisdr.org/campaign/resilientcities/uploads/city/attachments/3871-10684.pdf

[45]   ACI 318-19 requisitos de Reglamento de Construcción para Concreto Estructural ya disponible, Comité American Concrete Institute (ACI) 318, American Concrete Institute, Indiana, Estados Unidos, 2019. [Online]. Available: https://www.prnewswire.com/news-releases/aci-318-19-requisitos-de-reglamento-de-construccion-para-concreto-estructural-ya-disponible-866732703.html

[46]   C. Lampris, R. Lupo, and C. R. Cheeseman, "Geopolymerisation of silt generated from construction and demolition waste washing plants," *Waste Management*, vol. 29, no. 1, pp. 368–373, Jan. 2009. https://doi.org/10.1016/j.wasman.2008.04.007

[47]   N. Cristelo, A. Fernández-Jiménez, C. Vieira, T. Miranda, and Á. Palomo, "Stabilisation of construction and demolition waste with a high fines content using alkali activated fly ash," *Construction and Building Materials,* vol. 170, pp. 26–39, May. 2018. https://doi.org/10.1016/j.conbuildmat.2018.03.057

[48]   A. de Rossi, M. J. Ribeiro, J. A. Labrincha, R. M. Novais, D. Hotza, and R. F. P. M. Moreira, "Effect of the particle size range of construction and demolition waste on the fresh and hardened-state properties of fly ash-based geopolymer mortars with total replacement of sand," *Process Safety and Environmental Protection*, vol. 129, pp. 130–137, Sep. 2019. https://doi.org/10.1016/j.psep.2019.06.026

[49]   F. Farooq *et al.*, "Geopolymer concrete as sustainable material: A state of the art review," *Constr. Build. Mater.*, vol. 306, no. 124762, p. 124762, Nov. 2021. https://doi.org/10.1016/j.conbuildmat.2021.124762

[50]   B. Joseph, and G. Mathew, "Influence of aggregate content on the behavior of fly ash based geopolymer concrete," *Scientia Iranica*, vol. 19, no. 5, pp. 1188–1194, Oct. 2012. https://doi.org/10.1016/j.scient.2012.07.006

[51]   K. Neupane, and S. A. Hadigheh, "Sodium hydroxide-free geopolymer binder for prestressed concrete applications," *Construction and Building Materials,* vol. 293, p. 123397, Jul. 2021. https://doi.org/10.1016/j.conbuildmat.2021.123397

[52]   K. T. Nguyen, N. Ahn, T. A. Le, and K. Lee, "Theoretical and experimental study on mechanical properties and flexural strength of fly ash-geopolymer concrete," *Construction and Building Materials,* vol. 106, pp. 65–77, Mar. 2016. https://doi.org/10.1016/j.conbuildmat.2015.12.033

[53]   S. Malazdrewicz, K. Adam Ostrowski, and Ł. Sadowski, "Self-compacting concrete with recycled coarse aggregates from concrete construction and demolition waste – Current state-of-the art and perspectives," *Constr Build Mater*, vol., 370, p. 130702, Mar. 2023. https://doi.org/10.1016/j.conbuildmat.2023.130702

[54]   H. Sasanipour, and F. Aslani, "Durability properties evaluation of self-compacting concrete prepared with waste fine and coarse recycled concrete aggregates," *Construction and Building Materials,* vol. 236, p. 117540, Mar. 2020. https://doi.org/10.1016/j.conbuildmat.2019.117540

[55]   A. Katz, "Properties of concrete made with recycled aggregate from partially hydrated old concrete," *Cement and Concrete Research*, vol. 33, no. 5, pp. 703–711, May 2003. https://doi.org/10.1016/S0008-8846(02)01033-5

[56]   S. C. Kou, and C. S. Poon, "Properties of self-compacting concrete prepared with coarse and fine recycled concrete aggregates," *Cement and Concrete Composites,* vol. 31, no. 9, pp. 622–627, Oct. 2009. https://doi.org/10.1016/j.cemconcomp.2009.06.005

[57]   Z. J. Grdic, G. A. Toplicic-Curcic, I. M. Despotovic, and N. S. Ristic, "Properties of self-compacting concrete prepared with coarse recycled concrete aggregate," *Construction and Building Materials,* vol. 24, no. 7, pp. 1129–1133, Jul. 2010. https://doi.org/10.1016/j.conbuildmat.2009.12.029

[58]   NTC 4076, Unidades de concreto para mampostería no estructural, ICONTEC - Instituto Colombiano de Normas Técnicas, Bogotá, Colombia, 2017. [Online]. Available: https://tienda.icontec.org/gp-unidades-de-concreto-para-mamposteria-no-estructural-ntc4076-2017.html

[59]   S. Merabti, S. Kenai, R. Belarbi, and J. Khatib, "Thermo-mechanical and physical properties of waste granular cork composite with slag cement," *Construction and Building Materials,* vol. 272, p. 121923, Feb. 2021. https://doi.org/10.1016/j.conbuildmat.2020.121923